Communication

Computational Studies on the A Cluster of Acetyl-Coenzyme A Synthase: Geometric and Electronic Properties of the NiFeC Species and Mechanistic Implications

Ralph P. Schenker, and Thomas C. Brunold

J. Am. Chem. Soc., **2003**, 125 (46), 13962-13963• DOI: 10.1021/ja037893q • Publication Date (Web): 28 October 2003

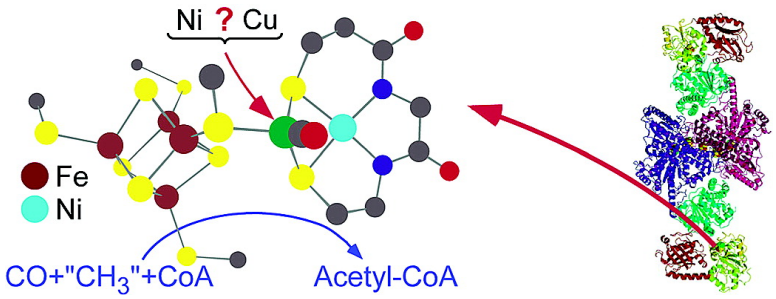

More About This Article

Additional resources and features associated with this article are available within the HTML version:

- Supporting Information
- Links to the 3 articles that cite this article, as of the time of this article download
- Access to high resolution figures
- Links to articles and content related to this article
- Copyright permission to reproduce figures and/or text from this article

View the Full Text HTML

J|A|C|S
COMMUNICATIONS

Published on Web 10/28/2003

Computational Studies on the A Cluster of Acetyl-Coenzyme A Synthase: Geometric and Electronic Properties of the NiFeC Species and Mechanistic Implications

Ralph P. Schenker and Thomas C. Brunold*

Department of Chemistry, University of Wisconsin-Madison, Madison, Wisconsin 53706

Received August 12, 2003; E-mail: brunold@chem.wisc.edu

Acetyl-CoA synthase/CO dehydrogenase (ACS/CODH) is a bifunctional enzyme enabling acetogenic, methanogenic, and sulfate-reducing archea and bacteria to grow autotropically on H_2 and CO_2.[1] The enzyme from the acetogen *Moorella thermoacetica* has been the subject of numerous enzymatic,[2] kinetic,[3] and spectroscopic[4−7] studies. The reaction catalyzed by ACS, conducted at the so-called A cluster, comprises the formation of acetyl-CoA from coenzyme A, CO, and a methyl group provided by a methylated corrinoid protein. The A cluster is stable in an oxidized state, a reduced $S = 3/2$ state, and a CO-bound, one-electron reduced $S = 1/2$ state. This latter A cluster form has been studied extensively by EPR,[5] Mössbauer,[6] and ENDOR[7] spectroscopies. It is called the NiFeC species, because incorporation of ^{61}Ni or ^{57}Fe as well as reaction with ^{13}CO all cause nuclear hyperfine broadening of the corresponding EPR signal.[5] Two recent X-ray crystallographic studies revealed that the A cluster consists of a $[Fe_4S_4]$ unit linked via a cysteine bridge to a proximal metal that in turn is connected to a square-planar, distal Ni site via two cysteine bridges (Figure 1). In the Doukov et al. structure,[8] the proximal site contains Cu and is tetrahedrally coordinated. In the Darnault et al. structure,[9] it is occupied by either Ni or Zn, with Ni partially occupying two distinct sites with approximate square-planar and tetrahedral geometries. Evidence has been presented supporting both the Cu[10] and Ni[9,11] forms of the A cluster to be catalytically relevant. Thus, despite these recent advances in ACS research, the nature of the catalytically active form of the A cluster and the potential catalytic role of the NiFeC species remain highly controversial. Here we use published spectroscopic data for the NiFeC species to evaluate possible A cluster models within the framework of density functional theory (DFT) calculations. Comparison of experimental and calculated hyperfine parameters reveals that the NiFeC species is associated with the Ni form.

Mössbauer studies by Münck and co-workers revealed that the NiFeC species features the $[Fe_4S_4]$ unit in the 2+ oxidation state and hinted toward the presence of Ni^+,[6b] consistent with the large observed ^{61}Ni hyperfine broadening. Thus, two potential models for the NiFeC species emerge: A $[Fe_4S_4]^{2+}-Ni_p{}^+CO-Ni_d{}^{2+}$ model (**1**) in which the proximal site is occupied by a Ni^+ ion that carries the $S = 1/2$ spin and a $[Fe_4S_4]^{2+}-Cu_p{}^+CO-Ni_d{}^+$ model (**2**) in which it is occupied by a diamagnetic Cu^+ ion while the spin resides on the distal Ni^+ atom. To evaluate those two possibilities, DFT computations[12] were carried out on A cluster models in which the $[Fe_4S_4]$ cysteinyl residues were replaced by methyl thiolates and the protein backbone coordinating the distal Ni atom was truncated as shown in Figure 1. Initial atomic positions were taken from ref 8 and subsequently optimized by DFT energy minimization. To account for the constraints imposed by the protein backbone, the C atomic positions represented by ● in Figure 1 were kept frozen.

Table 1 shows that optimized key interatomic distances for both models **1** and **2** are generally in good agreement with corresponding

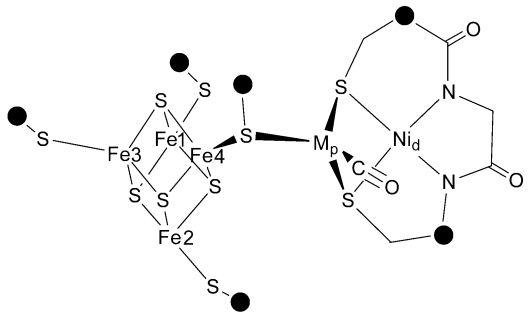

Figure 1. Schematic representation of the computational models employed. M_p denotes the proximal Ni and Cu for models **1** and **2**, respectively. C atoms represented by ● were kept frozen during geometry optimization.

Table 1. Comparison of Key Interatomic Distances (in Å) and Isotropic Hyperfine Parameters A_{iso} (in MHz) for Models **1** and **2**

	experimental	1	2
M_p-S	2.25[a]	2.31	2.39
Ni_d-S	2.20[b]	2.21	2.21
Ni_d-N	1.87[b]	1.91	1.91
M_p-Ni_d	2.65[a]	2.60	2.84
$A_{iso}(^{57}Fe1)$	−34.2[c]/−32.2[d]	−21.9	−25.6
$A_{iso}(^{57}Fe2)$	−34.2[c]/−32.2[d]	−21.4	−26.4
$A_{iso}(^{57}Fe3)$	+26.8[c]/+27.8[d]	+23.3	+22.5
$A_{iso}(^{57}Fe4)$	+26.8[c]/+27.8[d]	+23.7	+22.5
$A_{iso}(M_p)$	24.3[e] (Ni)	+17.1 (Ni)	−35.8 (Cu)
$A_{iso}(^{13}C)$	27.5[e]	+8.6	−4.1
$A_{iso}(^{61}Ni_d)$	N/A	−2.6	+0.7

[a] Cu EXAFS study.[10] [b] Ni EXAFS study on phen-treated isolated α subunit.[13] [c] Mössbauer study on isolated α subunit.[6b] [d] Mössbauer study on full enzyme.[6a] [e] ENDOR study on full enzyme.[7]

EXAFS data,[10,13,14] indicating that structural data alone do not permit discrimination between the two models. Nuclear hyperfine parameters for ^{57}Fe, ^{61}Ni, and ^{13}CO were therefore computed on the optimized geometries using the BP86/ZORA approach[12,15] and compared to those obtained from Mössbauer and ENDOR studies.[6,7] As for both models the calculated $A_{iso}(^{57}Fe)$ couplings are consistent with experimental data (Table 1), comparison of the computed $A_{iso}(^{61}Ni)$ values is of particular interest. In both models **1** and **2** the proximal metal site, occupied by Ni and Cu, respectively, produces large A_{iso} values, whereas the distal Ni_d site shows negligible isotropic ^{61}Ni hyperfine couplings (Table 1). Consequently, while for model **1** agreement with the experimental $A_{iso}(^{61}Ni)$ value is good,[16] for model **2** it is poor. Also, the calculated $A_{iso}(^{13}C)$ agrees substantially better with the experimental value for **1** than for **2**.[17]

These results are understood in terms of the different electronic structures of **1** and **2**. As expected, **1** formally consists of a diamagnetic $[Fe_4S_4]^{2+}$ unit linked to a Ni^+ ion that predominantly carries the $S = 1/2$ spin (unpaired spin density $s = +0.428$). This

10.1021/ja037893q CCC: $25.00

spin is partially delocalized onto the $[Fe_4S_4]^{2+}$ moiety ($s = +0.204$), generating the nonzero ^{57}Fe hyperfine interactions. The computations on model **2**, however, did not result in a $[Fe_4S_4]^{2+}-Cu_p^{+}CO-Ni_d^{+}$ cluster. Instead, the $[Fe_4S_4]$ moiety is formally reduced to the +1 state while the Ni_d remains oxidized in the 2+ state, as deprotonated amides favor high metal oxidation states.[9] This results in spin densities on C ($s = -0.002$) and Ni_d ($s = +0.009$) being too small to generate sizable hyperfine splittings.[18] The large values for $A_{iso}(^{57}Fe)$ are due to the $S = 1/2$ spin now being primarily localized on $[Fe_4S_4]^{+}$ and, to a small extent, on Cu_p.[18]

Together, our results indicate that the NiFeC species is best described as $[Fe_4S_4]^{2+}-Ni_p^{+}CO-Ni_d^{2+}$.[19] Further support for this conclusion is provided by the computed exchange parameter J for the antiferromagnetic coupling between Ni_p and the adjacent Fe4; our value of +120 cm^{-1} is in excellent agreement with the experimental $J = +100$ cm^{-1}.[6b,20] Therefore, our results provide convincing evidence that the NiFeC species contains Ni rather than Cu at the proximal metal site. Because the NiFeC EPR signal intensity parallels enzymatic activity,[11] our computational results also imply that the catalytically active ACS form contains Ni at the proximal metal site. Consequently, they do not support the "paramagnetic" mechanistic proposal[10] in which the NiFeC species is thought to contain Cu_p^{+} and Ni_d^{+} ions and to be catalytically relevant but are in line with the "diamagnetic" reaction mechanism[9] in which M_p is occupied by Ni. In this latter mechanistic proposal, the NiFeC species is not directly involved; instead, a reduced state A_{red2} featuring a Ni_p^{0} center was proposed to be the key reactive species.[9] To explore the feasibility of such a Ni_p^{0} center, we also performed computations on a $[Fe_4S_4]^{2+}-Ni_p^{0}-Ni_d^{2+}$ model (**3**).[21] Interestingly, our results indicate that the $[Fe_4S_4]$ unit becomes reduced to the +1 oxidation state while Ni_p is oxidized to Ni^{+}. Because the $[Fe_4S_4]$ unit is considered to remain in the same oxidation state during catalysis after A_{red2} formation,[9] such a reduced $[Fe_4S_4]^{+}$ unit is feasible. The $S = 1/2$ spins on the $[Fe_4S_4]$ unit ($s = +0.753$) and Ni_p ($s = -0.535$) couple antiferromagnetically to afford an overall diamagnetic cluster, in agreement with experimental data.[2b] Calculations were also performed on a truncated model (**3a**) of A_{red2} in which the $[Fe_4S_4]$ unit was replaced by a proton. Notably, this model adopts a diamagnetic ground state of the form $Ni_p^{0}-Ni_d^{2+}$, indicating that such a charge distribution would indeed be conceivable. However, after optimizing the geometry of this $Ni_p^{0}-Ni_d^{2+}$ moiety and reintroducing the $[Fe_4S_4]$ unit, the $[Fe_4S_4]^{+}-Ni_p^{+}-Ni_d^{2+}$ description was restored. These findings indicate that (i) the calculated electronic structure does not depend on the initial local geometry around the Ni_p site and (ii) the $[Fe_4S_4]^{2+}$ cluster is more easily reduced than Ni_p^{+}. In the ACS protein, the redox potential of the $[Fe_4S_4]^{2+/1+}$ couple is presumably raised further by the presence of hydrogen bonds to the cysteinyl ligands. Because our models are based on the closed conformation of the α subunit presumed to be relevant for the A_{red2} state,[9] our results indicate that this reactive A cluster form is better described as $[Fe_4S_4]^{+}-Ni_p^{+}-Ni_d^{2+}$ than as $[Fe_4S_4]^{2+}-Ni_p^{0}-Ni_d^{2+}$, provided that no major structural changes occur upon A cluster reduction. The presence of Ni_p^{+} in the A_{red2} state would hint toward a Ni_p^{+}/Ni_p^{3+} redox couple instead of Ni_p^{0}/Ni_p^{2+} being involved in methylation, as proposed for the related enzyme acetyl-CoA decarboxylase/synthase.[22]

Acknowledgment. R.P.S. gratefully acknowledges a postdoctoral fellowship from the Swiss National Science Foundation. T.C.B. thanks the University of Wisconsin-Madison for generous support. The authors thank Drs. Stephen Ragsdale and Javier Seravalli for helpful discussions.

Supporting Information Available: Computational details, atomic coordinates of the optimized geometries (Tables S1 and S3), and key computational results (Tables S2 and S4) of models **1** and **2** and computational results on models **3** (Tables S5 and S6) and **3a** (Tables S7 and S8) (PDF). This material is available free of charge via the Internet at http://pubs.acs.org.

References

(1) (a) Ferry, J. G. *Crit. Rev. Biochem. Mol. Biol.* **1992**, *27*, 473−503. (b) Ragsdale, S. W.; Kumar, M. *Chem. Rev.* **1996**, *96*, 2515−2540. (c) Lindahl, P. A. *Biochemistry* **2002**, *41*, 2097−2105.
(2)) (a) Xia, J.; Sinclair, J. F.; Baldwin, T. O.; Lindahl, P. A. *Biochemistry* **1996**, *35*, 1965−1971. (b) Barondeau, D. P.; Lindahl, P. A. *J. Am. Chem. Soc.* **1997**, *119*, 3959−3970. (c) Russel, W. K.; Lindahl, P. A. *Biochemistry* **1998**, *37*, 10016−10026.
(3) (a) Gorst, C. M.; Ragsdale, S. W. *J. Biol. Chem.* **1991**, *266*, 20687−20693. (b) Maynard, E. L.; Lindahl, P. A. *Biochemistry* **2001**, *40*, 13262−13267. (c) Maynard, E. L.; Sewell, C.; Lindahl, P. A. *J. Am. Chem. Soc.* **2001**, *123*, 4697−4703. (d) Tan, X. S.; Sewell, C.; Lindahl, P. A. *J. Am. Chem. Soc.* **2002**, *124*, 6277−6284.
(4) Cramer, S. P.; Eidsness, M. K.; Pan, W.-H.; Morton, T. A.; Ragsdale, S. W.; DerVartanian, D. V.; Ljungdahl, L. G.; Scott, R. A. *Inorg. Chem.* **1987**, *26*, 2477−2479.
(5) (a) Ragsdale, S. W.; Wood, H. G.; Antholine, W. E. *Proc. Natl. Acad. Sci. U.S.A.* **1985**, *82*, 6811−6814. (b) Lindahl, P. A.; Münck, E.; Ragsdale, S. W. *J. Biol. Chem.* **1990**, *265*, 3873−3879.
(6) (a) Lindahl, P. A.; Ragsdale, S. W.; Münck, E. *J. Biol. Chem.* **1990**, *265*, 3880−3888. (b) Xia, J.; Hu, Z.; Popescu, C. V.; Lindahl, P. A.; Münck, E. *J. Am. Chem. Soc.* **1997**, *119*, 8301−8312.
(7) Fan, C. L.; Gorst, C. M.; Ragsdale, S. W.; Hoffman, B. M. *Biochemistry* **1991**, *30*, 431−435.
(8) Doukov, T. I.; Iverson, T. M.; Seravalli, J.; Ragsdale, S. W.; Drennan, C. L. *Science* **2002**, *298*, 567−572.
(9) Darnault, C.; Volbeda, A.; Kim, E. J.; Legrand, P.; Vernède, X.; Lindahl, P. A.; Fontecilla-Camps, J. C. *Nat. Struct. Biol.* **2003**, *10*, 271−279.
(10) Seravalli, J.; Gu, W.; Tam, A.; Strauss, E.; Begley, T. P.; Cramer, S. P.; Ragsdale, S. W. *Proc. Natl. Acad. Sci. U.S.A.* **2003**, *100*, 3689−3694.
(11) Bramlett, M. R.; Tan, X.; Lindahl, P. A. *J. Am. Chem. Soc.* **2003**, *125*, 9316−9317.
(12) For computational details, see Supporting Information.
(13) Russel, W. K.; Stålhandske, C. M. V.; Xia, J.; Scott, R. A.; Lindahl, P. A. *J. Am. Chem. Soc.* **1998**, *120*, 7502−7510.
(14) In the as-isolated ACS samples used for the EXAFS studies in ref 10, no CO is bound to the Cu ion. It can be expected that the Cu−S bonds would lengthen upon CO binding, which could at least partly explain the difference between the average experimental Cu−S distance and the one obtained for model **2**.
(15) Because computation of g values using the ZORA method[12] is limited to $S = 1/2$ systems and cannot be employed in conjunction with spin-unrestricted wave functions, the presence of the exchange-coupled $[Fe_4S_4]^{2+}$ unit prevented us from computing meaningful g values.
(16) The fact that only one of the two Ni ions in model **1** exhibits sizable hyperfine coupling is in line with the finding in ref 7 that a single Ni atom was sufficient to simulate the ENDOR spectra.
(17) Because the spin density on C is determined by the orientation of the CO ligand with respect to the Ni_p^{+} 3d orbital containing the single unpaired electron, the magnitude of $A_{iso}(C)$ critically depends on the geometry around the Ni_p center and is thus difficult to predict quantitatively (see Craft, J. L.; Mandimutsira, B. S.; Fujita, K.; Riordan, C. G.; Brunold, T. C. *Inorg. Chem.* **2003**, *42*, 859−867).
(18) In accordance with the formal Cu^{+} oxidation state, the spin density on Cu in model **2** is quite small ($s = -0.012$). The larger calculated value for $A_{iso}(^{63}Cu)$ than for $A_{iso}(^{61}Ni)$ (Table 1) thus mainly reflects the much larger nuclear g value of $g_n(^{63}Cu) = +1.48$ compared to $g_n(^{61}Ni) = -0.50$.
(19) The computed average Mössbauer ^{57}Fe quadrupole splittings are found to be $\Delta E_Q = +1.02$ mm/s for **1** but $\Delta E_Q = +1.55$ mm/s for **2** using a value of $Q = 0.21$ barn for the nuclear quadrupole moment (see Gütlich, P.; Link, R.; Trautwein, A. *Mössbauer Spectroscopy and Transition Metal Chemistry*; Springer: Berlin, 1978; Chapter 7, Table 7.1.). Thus, model **1** is in better agreement with previously reported experimental values $\Delta E_Q = 1.15$ mm/s[6a] and $\Delta E_Q = 1.21$ mm/s.[6b]
(20) These values are based on the model Hamiltonian $\mathbf{H} = J\,\mathbf{S}_{Ni}\cdot\mathbf{S}_{Fe34} + J_{cube}\,\mathbf{S}_{Fe12}\cdot\mathbf{S}_{Fe34}$, in which $S_{Ni} = 1/2$ and S_{Fe12}, $S_{Fe34} = 9/2$. See Supporting Information for details.
(21) Model **3** was generated from optimized model **1** by removal of the CO ligand and subsequent geometry optimization using the same constraints as for **1** and **2**. Key computational results are shown in Tables S5 and S6.
(22) Gencic, S.; Grahame, D. A. *J. Biol. Chem.* **2003**, *278*, 6101−6110.

JA037893Q